

A. Hinda, M. Khiat, Z. Boudjema

FUZZY SECOND ORDER SLIDING MODE CONTROL OF A UNIFIED POWER FLOW CONTROLLER

Purpose. This paper presents an advanced control scheme based on fuzzy logic and second order sliding mode of a unified power flow controller. This controller offers advantages in terms of static and dynamic operation of the power system such as the control law is synthesized using three types of controllers: proportional integral, and sliding mode controller and Fuzzy logic second order sliding mode controller. Their respective performances are compared in terms of reference tracking, sensitivity to perturbations and robustness. We have to study the problem of controlling power in electric system by UPFC. The simulation results show the effectiveness of the proposed method especially in chattering-free behavior, response to sudden load variations and robustness. All the simulations for the above work have been carried out using MATLAB / Simulink. Various simulations have given very satisfactory results and we have successfully improved the real and reactive power flows on a transmission line as well as to regulate voltage at the bus where it is connected, the studies and illustrate the effectiveness and capability of UPFC in improving power. References 25, tables 2, figures 10.

Key words: UPFC, FACTS, PI, second order sliding mode, fuzzy logic.

Цель. В настоящей статье представлена усовершенствованная схема управления, основанная на нечеткой логике и режиме скольжения второго порядка унифицированного контроллера потока мощности. Данный контроллер обладает преимуществами с точки зрения статической и динамической работы энергосистемы, например, закон управления синтезируется с использованием трех типов контроллеров: пропорционально-интегрального, контроллера скользящего режима и контроллера скользящего режима нечеткой логики второго порядка. Их соответствующие характеристики сравниваются с точки зрения отслеживания эталонов, чувствительности к возмущениям и надежности. Необходимо изучить проблему управления мощностью в энергосистеме с помощью унифицированного контроллера потока мощности (UPFC). Результаты моделирования показывают эффективность предложенного метода, особенно в отношении отсутствия вибрации, реакции на внезапные изменения нагрузки и устойчивости. Все расчеты для вышеуказанной работы были выполнены с использованием MATLAB/Simulink. Различные расчетные исследования дали весьма удовлетворительные результаты, и мы успешно улучшили потоки реальной и реактивной мощности на линии электропередачи, а также регулирование напряжения на шине, к которой она подключена, что позволяет изучить и проиллюстрировать эффективность и возможности UPFC для увеличения мощности. Библ. 25, табл. 2, рис. 10.

Ключевые слова: унифицированный контроллер потока мощности (UPFC), гибкая система передачи переменного тока (FACTS), PI (пропорционально-интегральный) контроллер, скользящий режим второго порядка, нечеткая логика.

Introduction. In recent years, the electrical power distribution system are suffering from significant power flow quality (PQ) problems, which are characterized by low power factor, poor voltage profile, voltage stability, load unbalancing, and supply interruptions. These power quality issues have attracted attention to the researchers both in academic and industry. As a result, many power quality standards were proposed in [1]. By the reason of these power quality issues, the use of flexible AC transmission system (FACTS) controllers in power system has been of worldwide interest for increasing the power transfer capability and enhancing power system controllability and stability due to their speed and flexibility. In addition, converter based FACTS controllers are capable of independently controlling both active and reactive power flow in the power system [2].

Unified power flow controller (UPFC) is the member of FACTS device. It is the most versatile and powerful FACTS device [3]. The fundamental theory of UPFC is that, the phase angle affects flow of real power and the magnitude of voltage affects flow of reactive power [4, 5].

This device consists of two other FACTS devices: the Static Synchronous Series Compensator (SSSC) and the Static Synchronous Compensator (STATCOM), the SSSC injects an almost sinusoidal voltage, of variable magnitude in series with the system voltage provides the most cost effective solution to mitigate voltage sags by improving power quality level that is required by customer and the STATCOM connected by a common DC link capacitor. It can simultaneously perform the

function of transmission line real/reactive power flow control in addition to UPFC bus voltage/shunt reactive power control [6].

Though UPFC implies many advantages, but its controller design still being a matter of challenge since it is a multi-variable controller. In literature, a lot of works have been presented with diverse control diagrams of UPFC for various power system applications. Recently, the sliding mode control (SMC) method has been widely used for robust control of nonlinear systems. Several papers have been published based on SMC of UPFC [7-9]. Nevertheless, the deficiency of this type of control, which is the chattering phenomenon caused by the discontinuous control action. To resolve this problem, several modifications to the usual control law have been proposed, the most popular being the boundary layer approach [10, 11].

Fuzzy logic is a technology based on engineering experience and observations. In fuzzy logic, an exact mathematical model is not necessary because linguistic variables are used to define system behavior rapidly. One way to improve sliding mode controller performance is to combine it with fuzzy logic to form a fuzzy sliding mode controller. The design of a sliding mode controller incorporating fuzzy control helps in achieving reduced chattering, simple rule base, and robustness against disturbances and nonlinearities.

This paper discusses the capability of UPFC on controlling independently the active and reactive power in

© A. Hinda, M. Khiat, Z. Boudjema

the power transmission line and the improvement of the transient and dynamic stability of the power system by the UPFC are examined. Active and reactive powers are controlled using three types of controllers: Proportional-Integral (PI) and SMC and Fuzzy logic second order sliding mode controller (FLSOSMC). Their performances are compared in terms of reference tracking, sensitivity to perturbations and robustness.

Structure of the UPFC. For many years, UPFC is considered as the most versatile of the FACTS device one that can be used to enhance steady state stability, dynamic stability and transient stability, which combines the good features of STATCOM and SSSC. Fig. 1 shows the basic structure of UPFC which consists of two voltage sourced converters (VSC) and used to provide galvanic isolation and adjust the voltage levels in the supply system. It is composed of two inverters with PWM control (Pulse Width Modulation), which are operated from a DC link provided by a dc storage capacitor. One is connected in parallel and the other in series with the transmission line [12]. The detailed structure and the functionality of the UPFC can be found in [13].

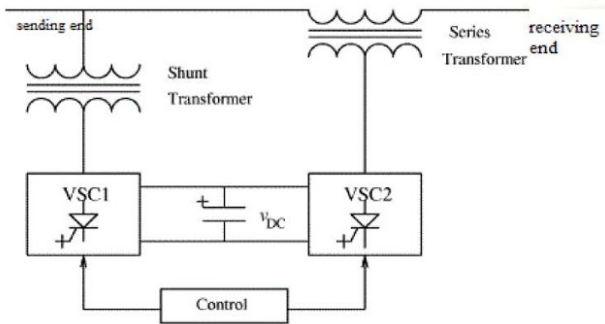


Fig. 1. Basic structure of the UPFC.

The modeling of the UPFC. Figure 2 represents the simplified model circuit of the UPFC.

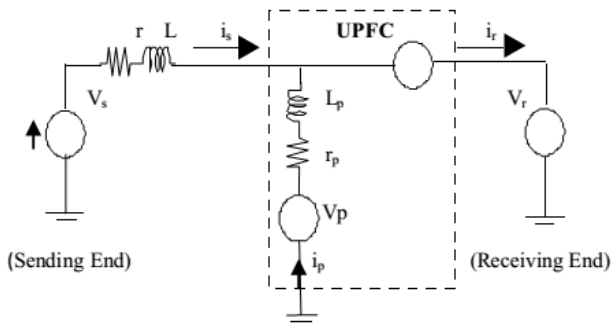


Fig. 2. Equivalent circuit of the UPFC

Applying Kirchhoff law on equivalent circuit shown in Fig. 2, the dynamic equations of the UPFC series branch is

$$\frac{d}{dt} \begin{bmatrix} I_{sa} \\ I_{sb} \\ I_{sc} \end{bmatrix} = \begin{bmatrix} -r/L & 0 & 0 \\ 0 & -r/L & 0 \\ 0 & 0 & -r/L \end{bmatrix} \begin{bmatrix} I_{sa} \\ I_{sb} \\ I_{sc} \end{bmatrix} + \begin{bmatrix} 1/L & 0 & 0 \\ 0 & 1/L & 0 \\ 0 & 0 & 1/L \end{bmatrix} \begin{bmatrix} V_{sa} - V_{ca} - V_{ra} \\ V_{sb} - V_{cb} - V_{rb} \\ V_{sc} - V_{cc} - V_{rc} \end{bmatrix} \quad (1)$$

Using Park transformation, the equations (1) will be written as

$$\frac{d}{dt} \begin{bmatrix} I_{sd} \\ I_{sq} \end{bmatrix} = \begin{bmatrix} -r/L & +\omega \\ -\omega & -r/L \end{bmatrix} \begin{bmatrix} I_{sd} \\ I_{sq} \end{bmatrix} + \begin{bmatrix} 1/L & 0 \\ 0 & 1/L \end{bmatrix} \begin{bmatrix} V_{sd} - V_{cd} - V_{rd} \\ V_{sq} - V_{cq} - V_{rq} \end{bmatrix} \quad (2)$$

The modeling of the UPFC shunt branch. The complete mathematical model of the UPFC shunt is given similarly by the following matrix

$$\frac{d}{dt} \begin{bmatrix} I_{pa} \\ I_{pb} \\ I_{pc} \end{bmatrix} = \begin{bmatrix} -r_p/L_p & 0 & 0 \\ 0 & -r_p/L_p & 0 \\ 0 & 0 & -r_p/L_p \end{bmatrix} \begin{bmatrix} I_{pa} \\ I_{pb} \\ I_{pc} \end{bmatrix} + \begin{bmatrix} 1/L_p & 0 & 0 \\ 0 & 1/L_p & 0 \\ 0 & 0 & 1/L_p \end{bmatrix} \begin{bmatrix} V_{pa} - V_{ca} - V_{ra} \\ V_{pb} - V_{cb} - V_{rb} \\ V_{pc} - V_{cc} - V_{rc} \end{bmatrix} \quad (3)$$

Since the system is assumed to be a balanced one, it can be transformed into a synchronous d-q-o frame by applying Park's transformation. The matrix form (3) is given as follows

$$\frac{d}{dt} \begin{bmatrix} I_{pd} \\ I_{pq} \end{bmatrix} = \begin{bmatrix} -r_p/L_p & +\omega \\ -\omega & -r_p/L_p \end{bmatrix} \begin{bmatrix} I_{pd} \\ I_{pq} \end{bmatrix} + \begin{bmatrix} 1/L_p & 0 \\ 0 & 1/L_p \end{bmatrix} \begin{bmatrix} V_{pd} - V_{cd} - V_{rd} \\ V_{pq} - V_{cq} - V_{rq} \end{bmatrix} \quad (4)$$

The modeling of the UPFC continues branch. For the DC-side circuit, based on the power balance equation in the output and input of UPFC, The net real power exchanged by both the converters through DC side should be zero to keep the capacitor voltage constant [14]. The DC voltage V_{dc} dynamics across the capacitor is given by the following equation

$$\frac{dV_{dc}}{dt} = \frac{1}{CV_{dc}} (P_e - P_{ep}), \quad (5)$$

where P_e – active power absorbed of the AC system

$$P_e = v_{ca} \cdot i_{sa} + v_{cb} \cdot i_{sb} + v_{cc} \cdot i_{sc};$$

where P_{ep} – active power injected by the shunt inverter AC system

$$P_{ep} = v_{pa} \cdot i_{pa} + v_{pb} \cdot i_{pb} + v_{pc} \cdot i_{pc}.$$

By performing Park transformation, the DC voltage V_{dc} dynamics across the capacitor can be described by the following equations

$$\frac{dV_{dc}}{dt} = \frac{1}{CV_{dc}} (v_{pd} \cdot I_{pd} + v_{pq} \cdot I_{pq} - v_{cd} \cdot I_{rd} - v_{cq} \cdot I_{rq}). \quad (6)$$

Control of the parallel converter. The ordinary working principle of the parallel compensation of STATCOM is described as follows: active power control which means stabilizing the capacitor voltage of the DC side; reactive power control which means stabilizing the terminal voltage [15]. According to the system of equations (2) the control strategy of parallel compensation (STATCOM) is decoupling of the two current loops control, to reduce the interaction between the active and reactive power. The control block diagram is shown in Fig. 3.

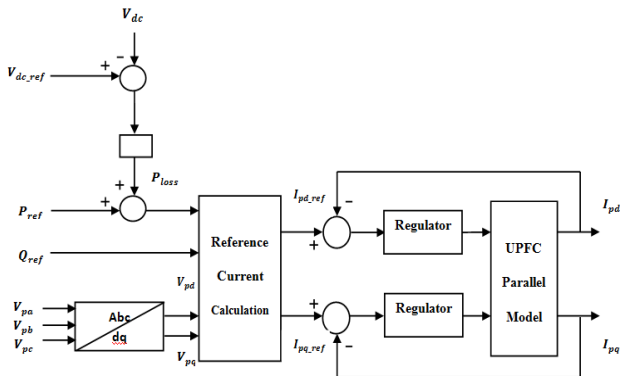


Fig. 3. Control system of shunt part

Control of the series converter. The SSSC regulate the active and reactive power flow on the transmission line where the UPFC is installed by injection voltage of which the amplitude and the phase both can be adjusted. The control strategy of the series compensator is decoupling of the two current loops control. The diagram of control circuits of SSSC is given in the Fig. 4.

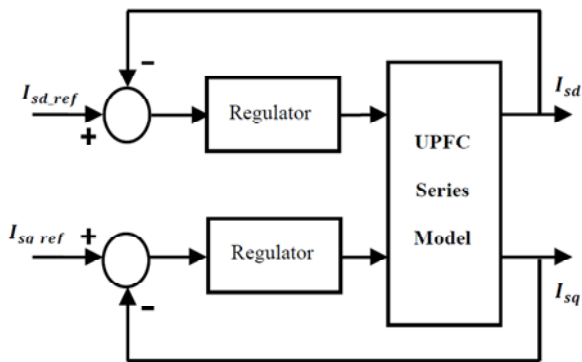


Fig. 4. Control system of series part

In this section, we have chosen to compare the performances of the UPFC with two different controllers: PI and SMC.

PI controller. This controller is simple to elaborate. Fig. 5 shows the block diagram of the system implemented with this controller. The terms k_p and k_i represent respectively the proportional and integral gains.

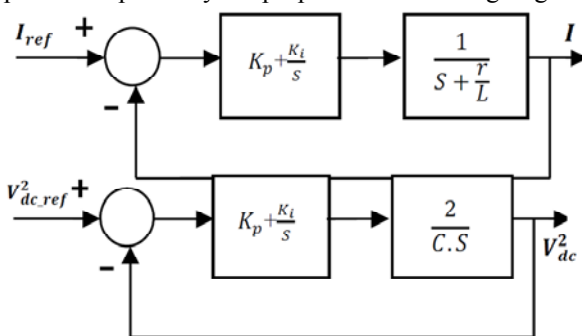


Fig. 5. System with PI controller

The regulator terms are calculated with a pole compensation method. The time response of the controlled system will be fixed at $\tau = 5$ ms. This value is sufficient for our application and a lower value might involve transients with important overshoots. The calculated terms are represented in Table 1.

Table 1

Optimal parameters of the proposed controllers			
	Controller series part	Controller shunt part	Controller continues branch
K_p	$1/\tau$	$1/\tau$	$C \cdot \omega^2/2$
K_i	$\left(\frac{R}{L}\right)K_p$	$\left(\frac{r_p}{L_p}\right)K_p$	$C \cdot \xi \omega$

It is important to specify that the pole compensation is not the only method to calculate a PI regulator but it is simple to elaborate with a first order transfer-function and it is sufficient in our case to compare with other regulators.

Sliding mode controller. Sliding mode control is one of the effective nonlinear robust control approaches since it provides system dynamics with an invariance property to uncertainties once the system dynamics are controlled in the sliding mode [16-18]. The main feature of Sliding mode controller (SMC) is that it only needs to drive the error to a switching surface it consists of three parts Fig. 6.

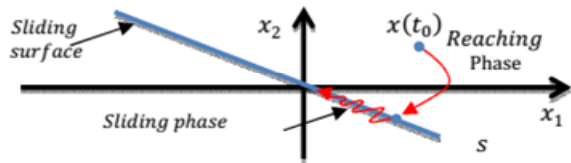


Fig. 6. Phase portrait of sliding mode control

The switching surface choice. The design of the control system will be demonstrated for a nonlinear system presented in the canonical form [17]:

$$\begin{cases} \dot{x} = f(x, t) + B(x, t) \cdot V(x, t); \\ x \in R^n, V \in R^m, \text{ran}(B(x, t)) = m, \end{cases} \quad (7)$$

where $f(x, t)$, $B(x, t)$ – two continuous and uncertain nonlinear functions, supposed limited.

We take the general equation to determine the sliding surface proposed by J.J. Slotine [20, 21] given by

$$S(X) = \left(\frac{d}{dt} + \lambda\right)^{n-1} e; \quad e = x^* - x, \quad (8)$$

where e – error on the signal to be adjusted; λ – a positive coefficient; n – system order; x^* – desired signal; x – state variable of the control signal.

Convergence condition. The convergence condition is defined by the Lyapunov equation [14]; it makes the surface attractive and invariant :

$$S \cdot \dot{S} < 0. \quad (9)$$

Control calculation. The control algorithm is defined by the relation [17]:

$$V^{com} = V^{eq} + V^n, \quad (10)$$

where V^{com} is the control vector, V^{eq} is the equivalent control vector, V^n is the correction factor and must be calculated so that the stability conditions for the selected control are satisfied

$$V^n = Ksat(S(X)/\delta), \quad (11)$$

$$sat(S(X)/\delta) = \begin{cases} sign(S) & \text{if } |S| > \delta; \\ S/\delta & \text{if } |S| < \delta; \end{cases} \quad (12)$$

where $\text{sat}(S(x)/\delta)$ is the proposed saturation function, δ is the boundary layer thickness.

In our study, the errors between the references and measured I_d and I_q currents have been chosen as sliding mode surfaces, so we can write the following expression

$$\begin{cases} s_d = I_{sd_ref} - I_{sd}; \\ s_q = I_{sq_ref} - I_{sq}. \end{cases} \quad (13)$$

The first order derivate of (8) gives

$$\begin{cases} \dot{s}_d = \dot{I}_{sd_ref} - \dot{I}_{sd}; \\ \dot{s}_q = \dot{I}_{sq_ref} - \dot{I}_{sq}. \end{cases} \quad (14)$$

Taking its derivative and replacing it in the current \dot{I}_{sd} and \dot{I}_{sq} expression (2) we get

$$\begin{cases} \dot{s}_d = \dot{I}_{sd_ref} - \omega I_{sq} + \frac{r}{L} I_{sd} - \frac{1}{L} (v_{sd} - v_{cd} - v_{rd}); \\ \dot{s}_q = \dot{I}_{sq_ref} + \omega I_{sd} + \frac{r}{L} I_{sq} - \frac{1}{L} (v_{sq} - v_{cq} - v_{rq}) \end{cases} \quad (15)$$

Replacing the expression of v_{cd} and v_{cq} in (10) by their expressions given in (15), one obtains

$$\begin{cases} \dot{s}_d = \dot{I}_{sd_ref} - \omega I_{sq} + \frac{r}{L} I_{sd} - \frac{1}{L} (v_{sd} - (v_{cd}^n + v_{cd}^{eq}) - v_{rd}); \\ \dot{s}_q = \dot{I}_{sq_ref} + \omega I_{sd} + \frac{r}{L} I_{sq} - \frac{1}{L} (v_{sq} - (v_{cq}^n + v_{cq}^{eq}) - v_{rq}) \end{cases} \quad (16)$$

I_{qr} will be the component of the control vector used to constraint the system to converge to $S=0$. The control vector v^{eq} is obtain by imposing $\dot{S}=0$ so the equivalent control components are given by the following relation

$$\begin{cases} v_{cd}^{eq} = -L\dot{I}_{sd_ref} + L\omega I_{sq} - rI_{sd} + v_{sd} - v_{rd}; \\ v_{cq}^{eq} = -L\dot{I}_{sq_ref} - L\omega I_{sd} - rI_{sq} + v_{sq} - v_{rq}. \end{cases} \quad (17)$$

Using the same procedures as for part shunt we get the following expression:

$$\begin{cases} v_{cd}^{eq} = -L_p \dot{I}_{pd_ref} + L_p \omega I_{pq} - r_p I_{pd} + v_{pd} - v_{rd}; \\ v_{cq}^{eq} = -L_p \dot{I}_{pq_ref} - L_p \omega I_{pd} - r_p I_{pq} + v_{pq} - v_{rq}. \end{cases} \quad (18)$$

To obtain good performances, dynamic an commutation around the surface, the control vector is imposed as follows [19]

$$v = v^{eq} + K \cdot \text{sign}(S). \quad (19)$$

The sliding mode will exist only if the following condition is met

$$S \cdot \dot{S} < 0. \quad (20)$$

Fuzzy logic second order sliding mode controller (FLSOSMC). The sliding mode control is a widely studied control scheme that provides robustness to certain disturbances and system uncertainties [7, 9] Nevertheless, a few drawbacks arise in its practical implementation, such as chattering phenomenon Such chattering has many negative effects in real world applications since it may damage the control actuator and excite the undesirable unmodeled dynamics In order to reduce the effects of these problems, second order sliding mode seems to be a very attractive solution [22].

This method generalizes the essential sliding mode idea by acting on the higher order time derivatives of the sliding manifold, instead of influencing the first time

derivative as it is the case in SMC, therefore reducing chattering and while preserving SMC advantages [23].

In order to ensure the active and reactive power convergence to their reference, a second order sliding mode control (SOSMC) is used. Considering the sliding mode surface given by (15), the following expression can be written:

$$\begin{cases} \dot{s}_d = \dot{I}_{sd_ref} - \omega I_{sq} + \frac{r}{L} I_{sd} - \frac{1}{L} (v_{sd} - v_{cd} - v_{rd}); \\ \ddot{S}_d = Y_1(t, x) + A_1(t, x)v_{cd}, \end{cases} \quad (21)$$

and

$$\begin{cases} \dot{s}_q = \dot{I}_{sq_ref} - \omega I_{sd} + \frac{r}{L} I_{sq} - \frac{1}{L} (v_{sq} - v_{cq} - v_{rq}); \\ \ddot{S}_q = Y_2(t, x) + A_2(t, x)v_{cq}, \end{cases} \quad (22)$$

where $Y_1(t, x)$, $Y_2(t, x)$, $A_1(t, x)$ and $A_2(t, x)$ – uncertain functions which satisfy

$$\begin{cases} Y_1 > 0, |Y_1| > \lambda_1, 0 < K_{m1} < A_2 < K_{M1}; \\ Y_2 > 0, |Y_2| > \lambda_2, 0 < K_{m2} < A_2 < K_{M2}. \end{cases}$$

Basing on the super twisting algorithm introduced by Levant in [24], the proposed high order sliding mode controller contains two parts [25]

$$v_{cd} = v_1 + v_2. \quad (23)$$

With

$$\begin{cases} v_1 = -k_1 \cdot \text{sign}(S_d); \\ v_2 = -l \cdot |S_1|^\gamma \cdot \text{sign}(S_d); \\ v_{cq} = w_1 + w_2 \end{cases} \quad (24)$$

and with

$$\begin{cases} w_1 = -k_2 \cdot \text{sign}(S_q); \\ w_2 = -l \cdot |S_q|^\gamma \cdot \text{sign}(S_q). \end{cases}$$

In order to ensure the convergence of the sliding manifolds to zero in finite time, the gains can be chosen as follows [25]

$$\begin{cases} k_i > \frac{\lambda_i}{K_{mi}} \\ l_i^2 \geq \frac{4\lambda_i}{K_{mi}^2} \cdot \frac{K_{Mi}(k_i + \lambda_i)}{K_{mi}(k_i - \lambda_i)}; \quad i = 1,2; \\ 0 < \gamma \leq 0.5. \end{cases}$$

In order to improve the SOSMC of the UPFC and more and more decrease the adverse effect caused by the *sign* function, we propose in this paper to use the (FLSOSMC).

For the proposed FLSOSMC, the universes of discourses are first partitioned into the seven linguistic variables NB, NM, NS, EZ, PS, PM, PB, triangular and trapezoidal membership functions are chosen to represent the linguistic variables for the inputs and outputs of the controllers.

The fuzzy labels used in this study are negative big (NB), negative medium (NM), negative small (NS), equal zero (EZ), positive small (PS), positive medium (PM) and positive big (PB).

These choices are described in Fig. 7.

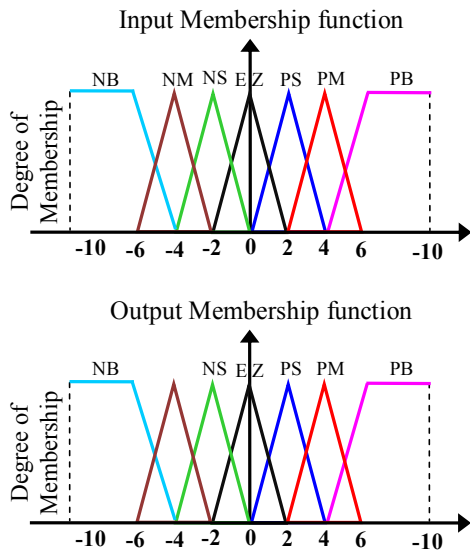


Fig. 7. Fuzzy sets and its memberships functions

Simulations and results. In this section, simulations are realized with a UPFC coupled to a 220V/50Hz grid. The system parameters are given in Table 2. The whole system is simulated using the Matlab/Simulink software.

Table 2
The parameters of the laboratory UPFC model

Parameter name	Symbol	Value	Unit
Network voltage	V_r	220	V
Voltage of the receiver	V_s	220	V
DC voltage	V_{dc}	280	V
Network frequency	f	50	HZ
The capacity of the common circuit DC	C	2	mF
Inductance 1	L	1.125	mH
Resistance 1	r	100	Ω
Inductance 2	L_p	1.125	mH
Resistance 2	r_p	100	Ω

In the objective to evaluate the performances of the controllers, three categories of tests have been realized: pursuit test, sensitivity to introducing perturbation and robustness facing variation of the reactance XL.

Pursuit test. This test has for goal the study of the three controllers (PI, SMC and FLSOSMC) behavior in reference tracking. The simulation results are presented in Fig. 8. As it's shown by this figure, for the 3 controllers, the active and reactive power track almost perfectly their references but with an important response time for the PI controller compared to the SMC and FLSOSMC. Therefore it can be considered that the two types of sliding mode controllers have a very good performance for this test.

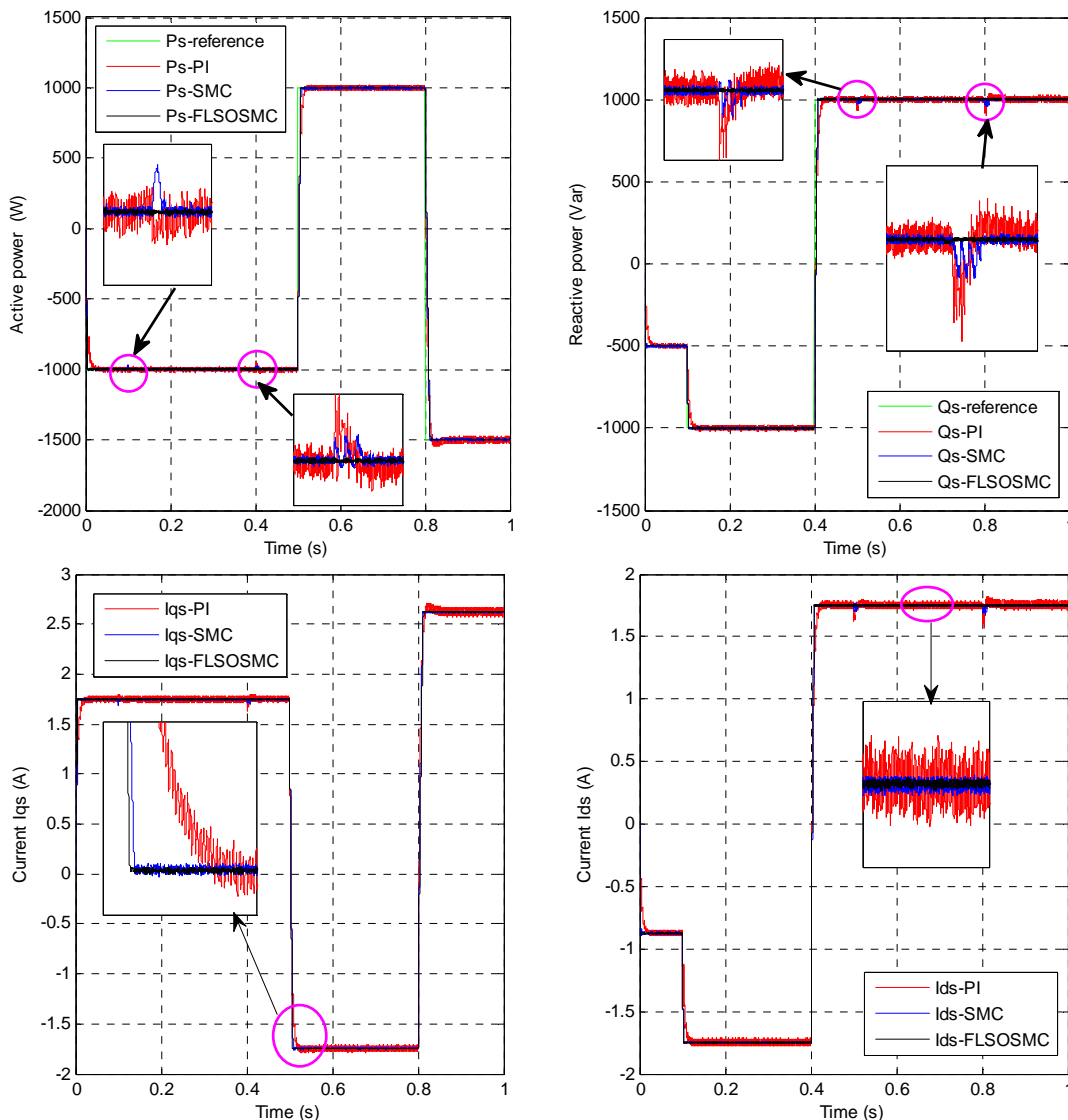


Fig. 8. Reference tracking test

Robustness. We tested the robustness of the used controllers for a variation of the reactance X_L . The results presented in Fig. 9 show that reactance variation presents a clear effect on the active and reactive powers of the two

used controllers and that the effect appears more significant for PI controller than that with the SMC and FLSOSMC. Thus it can be concluded that these last are robust against this parameter variation.

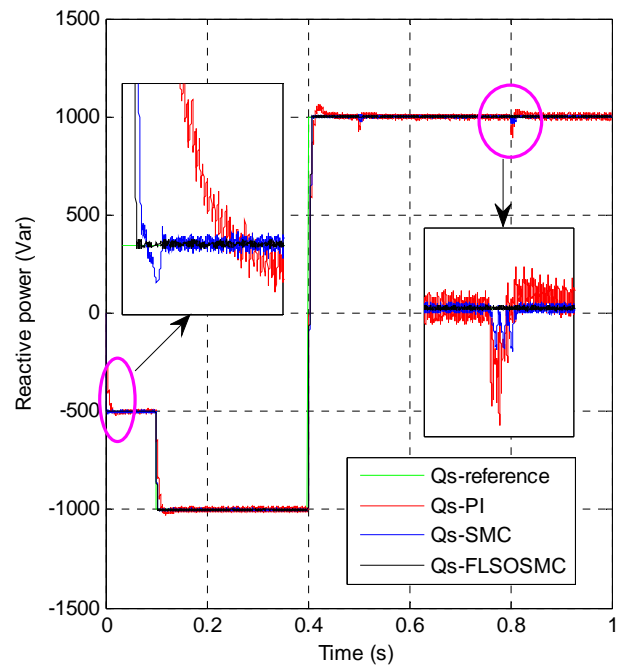
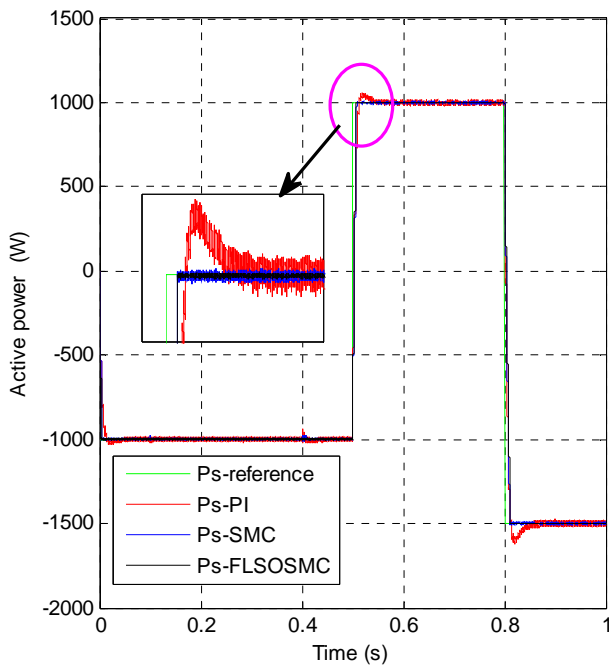


Fig. 9. Sensitivity to the reactance variation ($X_L -30\%$)

Sensitivity to a sub-voltage perturbation. The aim of this test is to analyze the influence of a sub-voltage perturbation (+50 %) in the time interval $t = 0.6$ s and $t = 0.62$ s on active and reactive powers for the 3 controllers. The simulation results are shown in Fig. 10. This figure expresses that the introducing perturbation

produced a slight effect on the power curves with PI controller. While the effects are almost negligible for the system with the two other controllers. This result is attractive for UPFC applications to ensure stability and quality of the active and reactive powers when the voltage is varying.

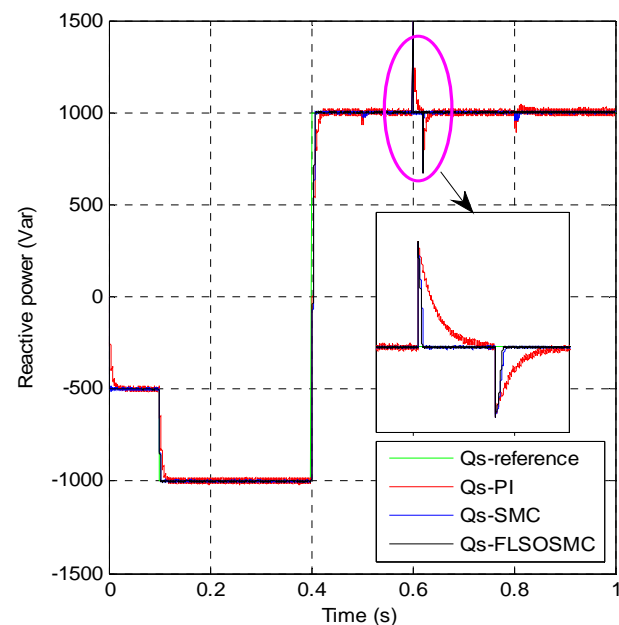
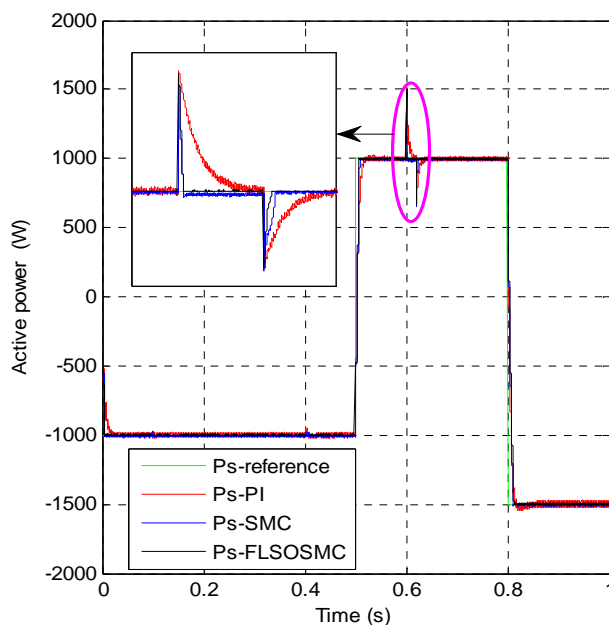


Fig. 10. Sensitivity to sub-voltage perturbation (+50 %)

Conclusion. A robust control method based on variable structure technique of a UPFC has been presented in this paper. Simulation results verified the effectiveness of the control strategy that allows independent control and decoupled active and reactive

power of these devices by minimizing the interaction effect between these powers. The Fuzzy logic second order sliding mode controller ensures a perfect decoupling between the two axes comparatively to the PI one where the coupling effect between them is very clear.

Results comparison between conventional PI Controller and the proposed Fuzzy logic second order sliding mode controller based controller for UPFC indicates that the proposed Fuzzy logic second order sliding mode controller based controller has less steeling time and less overshoot and compared with the conventional Proportional-Integral Controller.

Basing on all these results the UPFC device, can adjust the distribution the system power flow among the transmission line quickly and smoothly, and have no significant impact to other operating parameters of the system.

REFERENCES

1. IEEE Draft Recommended Practice for Monitoring Electric Power Quality. 2018.
2. Boudiaf M., Moudjahed M. Improvement of transient stability of power system by IPFC, SSSC and STATCOM. *Journal of Electrical Engineering*, 2014, vol.14, no.1, pp.257-272.
3. Yang S., Liu Y., Wang X., Gunasekaran D., Karki U., Peng F.Z. Modulation and Control of Transformerless UPFC. *IEEE Transactions on Power Electronics*, 2016, vol.31, no.2, pp. 1050-1063. doi: **10.1109/tpel.2015.2416331**.
4. Krishna T.M., Anjaneyulu K.S.R. Coordination of intelligent controllers for shunt and series converters of UPFC. *2015 Conference on Power, Control, Communication and Computational Technologies for Sustainable Growth (PCCCTSG)*, Dec. 2015. doi: **10.1109/pccctsg.2015.7503911**.
5. Round S.D. Performance of a unified power flow controller using a d-q control system. *Sixth International Conference on AC and DC Power Transmission*, 1996. doi: **10.1049/cp:19960384**.
6. Sharma N. K., Jagtap P.P. Modelling and Application of Unified Power Flow Controller (UPFC). *2010 3rd International Conference on Emerging Trends in Engineering and Technology*, 2010. doi: **10.1109/icetet.2010.169**.
7. Umre P.B., Bandal V.S., Dhamne A.R. Design of controller for Unified Power Flow Controller (UPFC) using Sliding Mode Control (SMC) strategies. *2014 5th International Conference – Confluence The Next Generation Information Technology Summit (Confluence)*, 2014. doi: **10.1109/CONFLUENCE.2014.6949286**.
8. Shotorbani A., Ajami A., Zadeh S., Aghababa M., Mahboubi B. Robust terminal sliding mode power flow controller using unified power flow controller with adaptive observer and local measurement. *IEEE IET Generation, Transmission & Distribution*, 2014, vol.8, no.10, p.1712-1723. doi: **10.1049/iet-gtd.2013.0637**.
9. Nayeripour M., Narimani M.S., Niknam T., Jam S. Design of sliding mode controller for UPFC to improve power oscillation damping. *Applied Soft Computing*, 2011, vol.11, no.8, 2011, pp. 4766-4772. doi: **10.1016/j.asoc.2011.07.006**.
10. López J., Sanchis P., Roboam X., Marroyo L. Dynamic Behavior of the Doubly Fed Induction Generator During Three-Phase Voltage Dips. *IEEE Transactions on Energy Conversion*, 2007, vol.22, no.3, pp. 709-717. doi: **10.1109/tec.2006.878241**.
11. Cupertino F., Naso D., Mininno E., Turchiano B. Sliding-Mode Control With Double Boundary Layer for Robust Compensation of Payload Mass and Friction in Linear Motors. *IEEE Transactions on Industry Applications*, 2009, vol.45, no.5, pp. 1688-1696. doi: **10.1109/tia.2009.2027521**.
12. Bouanane A., Amara M., Chaker A. State space neural network control (SSNNC) of UPFC for compensation power. *2015 3rd International Renewable and Sustainable Energy Conference (IRSEC)*, Dec. 2015. doi: **10.1109/irsec.2015.7455135**.
13. Kamel S., Jurado F., Lopes J.A.P. Comparison of various UPFC models for power flow control. *Electric Power Systems Research*, 2015, vol.121, pp. 243-251. doi: **10.1016/j.epsr.2014.11.001**.
14. Mallick R.K., Nahak N., Sinha R.R. Fuzzy sliding mode control for UPFC to improve transient stability of power system. *2015 Annual IEEE India Conference (INDICON)*, Dec. 2015. doi: **10.1109/indicon.2015.7443182**.
15. Meng W., Qinxiang G., Leiting C., Liqiang L., Caiyun Z. Mathematical Model and Control Strategy of UPFC. *2014 Sixth International Conference on Measuring Technology and Mechatronics Automation*, Jan. 2014. doi: **10.1109/icmtma.2014.96**.
16. Wai R.J., Chang J.M. Implementation of robust wavelet-neural-network sliding-mode control for induction servo motor drive. *IEEE Transactions on Industrial Electronics*, 2008, vol.50, no.6, pp. 1317-1334. doi: **10.1109/TIE.2003.819570**.
17. Utkin V.I. Sliding mode control design principles and applications to electric drives. *IEEE Transactions on Industrial Electronics*, 1993, vol.40, no.1, pp. 23-36. doi: **10.1109/41.184818**.
18. Astrom K.J., Wittenmark B. *Adaptive Control*. New York, Addison-Wesley, 1995.
19. Sun T., Chen Z., Blaabjerg F. Flicker study on variable speed wind turbines with doubly fed induction generators. *IEEE Transactions on Energy Conversion*, 2005, vol.20, no.4, pp.896-905. doi: **10.1109/TEC.2005.847993**.
20. Slotine J.J.E., Li W. *Applied Nonlinear Control*. Englewood Cliffs, NJ, Prentice-Hall, 1991.
21. Slotine J.-J.E. Sliding controller design for non-linear systems. *International Journal of Control*, 1984, vol.40, no.2, pp. 421-434. doi: **10.1080/00207178408933284**.
22. Tseng M.-L., Chen M.-S. Chattering reduction of sliding mode control by low-pass filtering the control signal. *Asian Journal of Control*, 2010, vol.12, no.3, pp. 392-398. doi: **10.1002/asjc.195**.
23. Boudjema Z., Meroufel A., Djerriri Y., Bounadja E. Fuzzy sliding mode control of a doubly fed induction generator for wind energy conversion. *Carpathian Journal of Electronic and Computer Engineering*, 2013, vol.6, no.2, pp. 7-14.
24. Levant A., Alelishvili L. Integral High-Order Sliding Modes. *IEEE Transactions on Automatic Control*, 2007, vol.52, no.7, pp. 1278-1282. doi: **10.1109/tac.2007.900830**.
25. Benelghali S., Benbouzid M.E.H., Charpentier J.F., Ahmed-Ali T., Munteanu I. Experimental Validation of a Marine Current Turbine Simulator: Application to a Permanent Magnet Synchronous Generator-Based System Second-Order Sliding Mode Control. *IEEE Transactions on Industrial Electronics*, 2011, vol.58, no.1, pp. 118-126. doi: **10.1109/tie.2010.2050293**.

Received 25.08.2019

Abdellatif Hinda¹, Associate Professor,
Mounir Khiaat¹, Doctor of Power Engineering, Professor,
Zinelaabidine Boudjema², Doctor of Power Engineering,
Professor,

¹ SCAMRE Laboratory,
Department of Electrical Engineering,
ENP Oran, Algeria.

² Electrical Engineering Department,
University of Chlef, Algeria,
e-mail: abdellatif.hinda2@gmail.com